

Vanda Grubišić*

Desert Research Institute, Reno, NV

and

Stephen A. Cohn

National Center for Atmospheric Research, Boulder, CO

1. INTRODUCTION

The Sierra Rotors Project (SRP) is a study of atmospheric rotors designed to establish quantitative characteristics of the rotor behavior in the lee of the Sierra Nevada including the rotor type, location and the frequency distribution of the related mountain-wave events, and to determine the extent to which current operational mesoscale models can reliably forecast the occurrence of rotors. The ground-based observing program of the Sierra Rotors Project (SRP) is being directed by the Desert Research Institute (DRI; Grubišić) in collaboration with the University of Washington (UW; Durran), the Naval Research Laboratory (NRL; Doyle), and the National Center for Atmospheric Research (NCAR; Kuettner). The Sierra Rotors Project is expected to yield new insight into the dynamics of rotors and their relation to the large-amplitude mountain waves and severe downslope wind events. This project represents the core of Phase I of the Terrain-induced Rotor Experiment (T-REX), a multi-year initiative focused on atmospheric rotors as well as low- and upper-level turbulence in airflow over complex terrain (Grubišić and Kuettner 2004).

The Special Observation Period (SOP) of SRP took place in March and April 2004 in Owens Valley, California. In this paper, we present preliminary analyses of some of the data collected during a strong wave and rotor event that had occurred during IOP 8 on 24–25 March 2004.

2. INSTRUMENTATION and DATA

The field site of the SRP was the central portion of Owens Valley south of Independence (Fig. 1). The Owens Valley is a narrow valley in eastern California, approximately north-south oriented and

bounded by the highest portion of the Sierra Nevada (High Sierra) to the west and by the White-Inyo Range to the east.

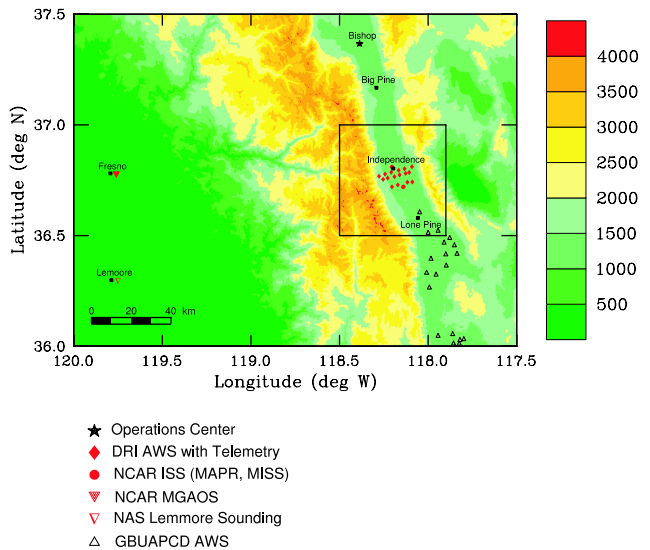


Figure 1: The Sierra Rotors Project field area with deployed ground instrumentation marked with red symbols.

The core of the instrumentation deployed in the SRP consist of the DRI network of 16 automatic weather stations (AWS) arranged in three approximately parallel rows. The average separation between individual stations along these three lines is approximately 3 km (Fig. 2). Each station consists of a standard 30 ft (10 m) meteorological tower, and sensors for wind, temperature, relative humidity, and pressure measurement. The stations' sensors are sampled every 3 seconds, and the data is temporally averaged over 30-second non-overlapping intervals. The temporally-averaged data are saved on the stations' data loggers before being sent via radio communication to the base station in Independence. From there, the data transfer to the central repository at DRI is carried over Internet, allowing near

*Corresponding author's address: Dr. Vanda Grubišić, Desert Research Institute, Division of Atmospheric Sciences, 2215 Raggio Pkwy, Reno, NV 89512-1095; e-mail: Vanda.Grubisic@dri.edu

real-time online access to the graphically-displayed data (<http://www.wrcc.dri.edu/trex/>).

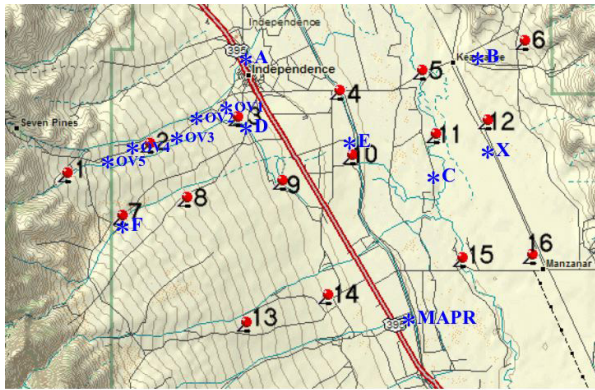


Figure 2: DRI AWS ground network layout. Blue stars mark the NCAR locations: MAPR site, MISS home site (A) as well as other identified MISS sites. Sites B, X, and OV5 were used during the SOP.

During SOP, the NCAR's Atmospheric Technology Division (ATD) Research Technology Facility (RTF) had deployed two Integrated Sounding Systems (ISS) in the Owens Valley. The two ISS are the Mobile Integrated Sounding System (MISS) and the Multiple Antenna Profiler/ISS (MAPR/ISS). MISS is a system similar to the Integrated Sounding System (ISS; Parsons et al. 1994) but with an additional ability to move more readily between locations (Cohn et al. 2004). MISS sensors include a 915 MHz boundary layer radar wind profiler, a Radio Acoustic Sounding System (RASS) for temperature profiling, and surface sensors for wind, temperature, relative humidity, and radiation, and a balloon-borne radiosonde sounding system. MAPR/ISS is a unique spaced antenna (SA) boundary layer wind profiler (Cohn et al. 2001) that measures the wind vector while pointing continuously in the vertical. The SA profilers provide a horizontal wind vector every few minutes (5-min is typical) and a vertical measurement every dwell (approximately 30 seconds). The home site for MISS was Independence airport (A), and MAPR was located just south of the main SRP AWS array (Fig. 2). All NCAR data were periodically transferred back to Boulder using a mobile internet satellite system, plotted, and displayed on the project web page (<http://www.atd.ucar.edu/rtf/projects/srp2004/>).

Given the importance of documenting the upstream thermodynamic and kinematic flow structure for interpreting the mountain wave response, substantial effort has been made to obtain adequate upwind upper-air sounding data. During

SOP, two supplemental upstream sounding sites were located in San Joaquin Valley. The mobile GPS atmospheric sounding system (MGAOS), part of the NCAR deployment, was based in Fresno, with an ability to change its position in order to be placed optimally for different upstream wind directions. The Naval Air Station (NAS) Lemoore (675 m ASL), which lies upwind of the area of interest under southwesterly winds was the other, fixed site. The rest of the instrumentation deployed during SOP is described in the companion paper by Grubišić and Kuettner (2004).

3. IOP 8 ROTOR EVENT

Sixteen Intensive Observation Periods (IOPs) were carried out during the two-month SOP. The first strong wave and rotor event of the SOP had occurred during IOP 8 on 24–25 March 2004. This is the case discussed in more detail in this paper.

3.a Synoptic Setting

The synoptic setting during IOP 8 was a classical prefrontal situation conducive of wave generation in Owens Valley. A deep low pressure center located off the coast of British Columbia, together with an attendant upper-level trough that had extended sufficiently far south, had produced strong south-westerly, cross-Sierra, flow at the ridge-height level and further aloft. Figure 3 shows the 36-h GFS forecast for winds, geopotential height, and vorticity at 500 hPa valid for 00 UTC on March 26 (-8 hours = 16 PST March 25). This system was forecasted to produce strong

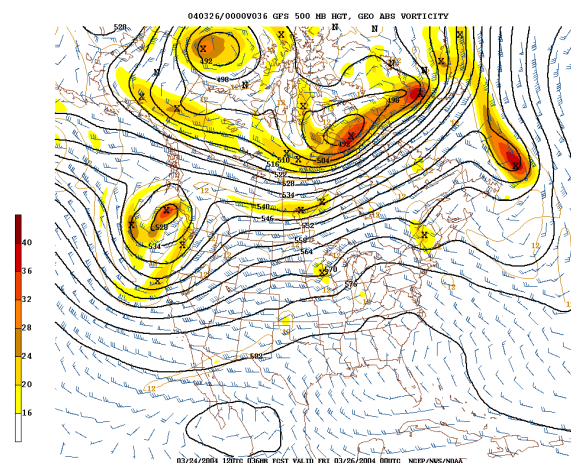


Figure 3: NCEP GFS model prediction for winds, geopotential height, and vorticity at 500 hPa for 00 UTC on March 26.

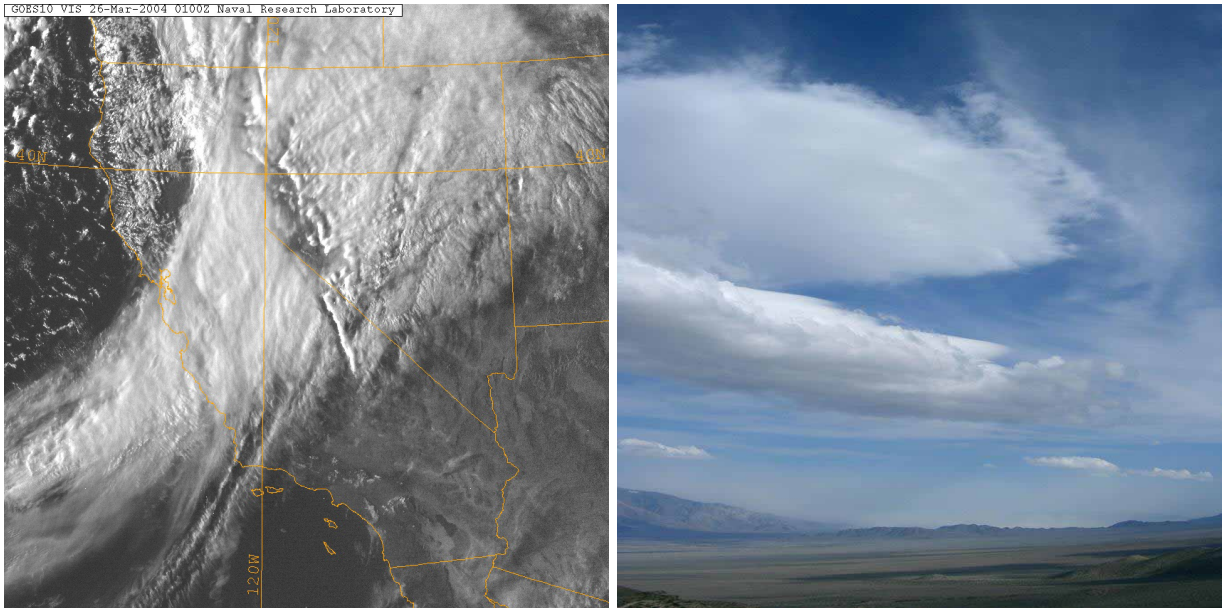


Figure 4: Left: GOES10 visible satellite image from 01 UTC March 26 (17 PST March 25). Right: A view from the ground of the roll (rotor) cloud underneath lenticular (wave) clouds around 17 PST March 25. Dust, lofted from the dry Owens Lake bed by strong westerly winds, is visible in the far south. View southeast from west of Independence. Photo by Vanda Grubišić.

cross-barrier flow for a period of several days. IOP 8 lasted from 18 UTC March 24 until 18 UTC March 26. The 24-hour period from 12 UTC March 25 to 12 UTC March 26 defines the core period of this IOP.

3.b Clouds: Satellite and Ground View

Sufficient amount of moisture was brought to the project area by this weather system to allow formation of wave clouds downwind of the Sierra Nevada. Figure 4 shows the GOES10 visible satellite image from 01 UTC on March 26 (17 PST March 25) revealing the presence of mountain wave clouds along the entire length of the Sierra Nevada. Particularly striking is the mountain wave cloud downwind of the High Sierra, recognizable as a bright linear cloud with a sharp upwind edge that is separated from a continuous upwind cloud deck by a foehn clearing (dark line). The right panel of this figure shows the view from the ground at approximately the same time, showing a substantial rotor cloud underneath wave clouds at higher levels.

3.c Ground Network Data

Figure 5 shows the time series of temperature, relative humidity, pressure, and wind direction, speed and gust recorded at stations 1 and 4 of

the ground network during a three-day period from 12 UTC (4 PST) March 24 to 12 UTC (4 PST) March 27 encompassing IOP 8. For reference, in the lower panels of the same figure, we show time series of the same physical quantities for a three day period of synoptically undisturbed weather. These two stations were selected as being representative of the gradually sloping terrain below the steep eastern Sierra slopes (station 1) and the middle flat part of the valley (station 4).

The IOP 8 event started around 20 UTC (12 PST) on March 24 with a sharp onset of westerly winds at both stations. Comparing the upper and lower panels of Fig. 5 reveals that during the entire three day period of 24–27 March the winds at both stations were highly disturbed, except during morning hours of March 25 when the wind regime shortly returned to the normal thermal circulation (with southerly winds in the middle of the valley and southeasterly on the gradual western slope) before turning back to the westerly or NW direction. We note also that the wind maxima during this three-day period occurred in the afternoon hours, which is more clearly evident in the station 4 record.

In the rest of this section, we focus on a 24-hour period from 12 UTC March 25 to 12 UTC March 26, during which a strong rotor was observed in the Owens Valley. The photo in Fig. 4 shows the roll (rotor) cloud (the line of cumulus) underneath

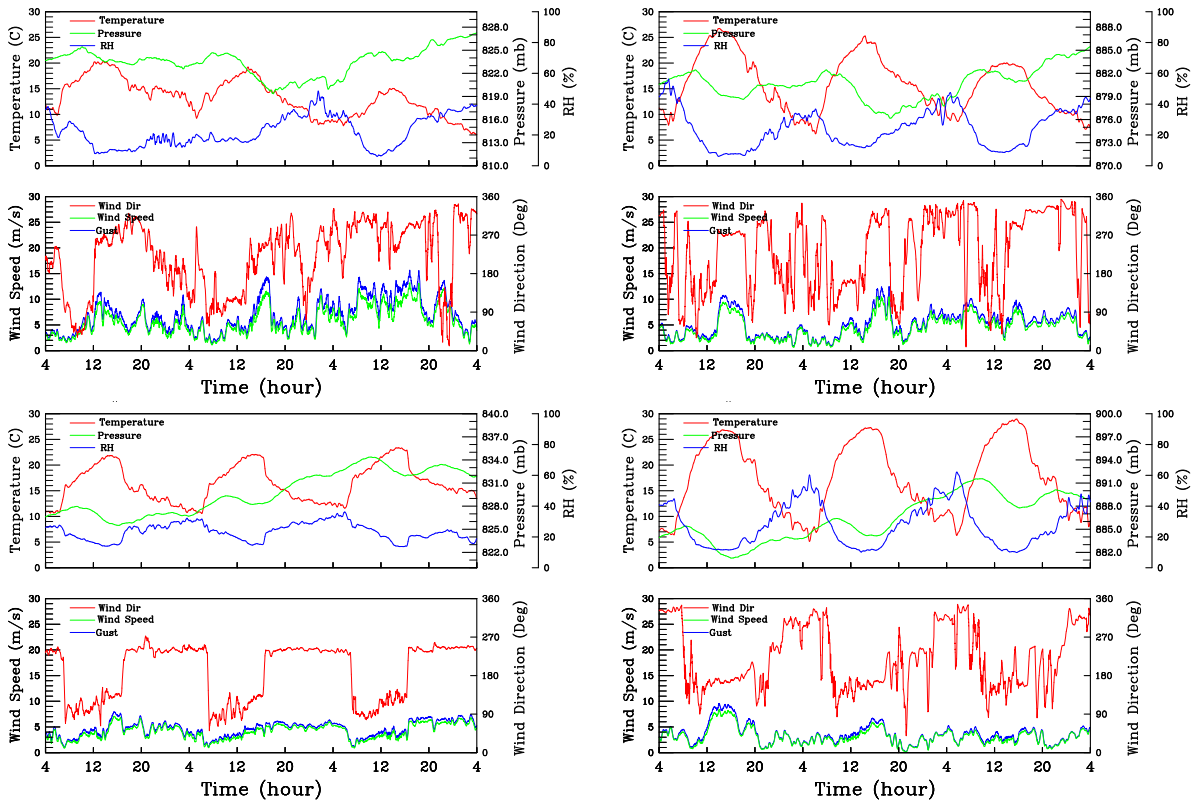


Figure 5: Time series plots of temperature, relative humidity, pressure and wind quantities measured at station 1 (left column) and station 4 (right column) of the ground network. Upper two panels: 12 UTC (4 PST) March 24 to 12 UTC March 27, 2004. Lower two panels: A three day period of calm weather illustrating an undisturbed thermal circulation pattern at these two stations. Times shown are PST.

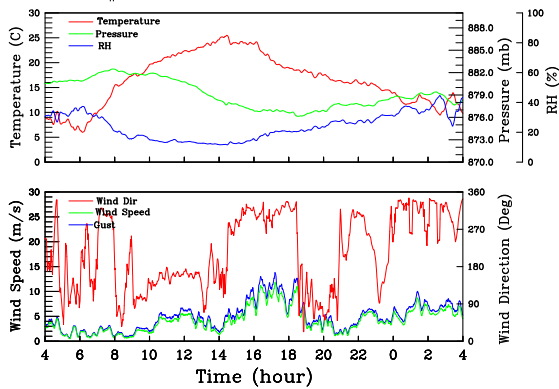


Figure 6: As in Fig. 5 but for station 4 for the period of 12 UTC (4 PST) March 25 to 12 UTC (4 PST) March 26. Times shown are PST.

lenticular (wave) clouds observed over the Owens Valley in the afternoon of March 25. As shown in the schematic in Fig. 7, if sufficiently strong, the rotor circulation under a crest of a mountain wave is expected to reach all the way to the ground, and

leave a footprint there. In Owens Valley, with the cross-barrier flow being westerly, the expected signature of a rotor are easterly winds on the ground. Zoom of the time series for station 4 for March 25 (Fig. 6) shows a two-hour period of easterly winds centered on 19 PST within a longer period of sustained northwesterly winds at this station.

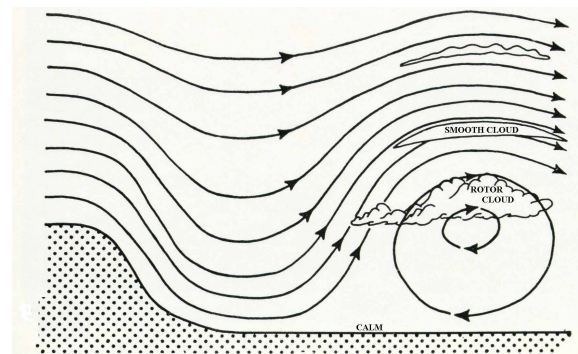


Figure 7: The schematic diagram of the two-dimensional airflow pattern with waves and rotors downwind of a ridge.

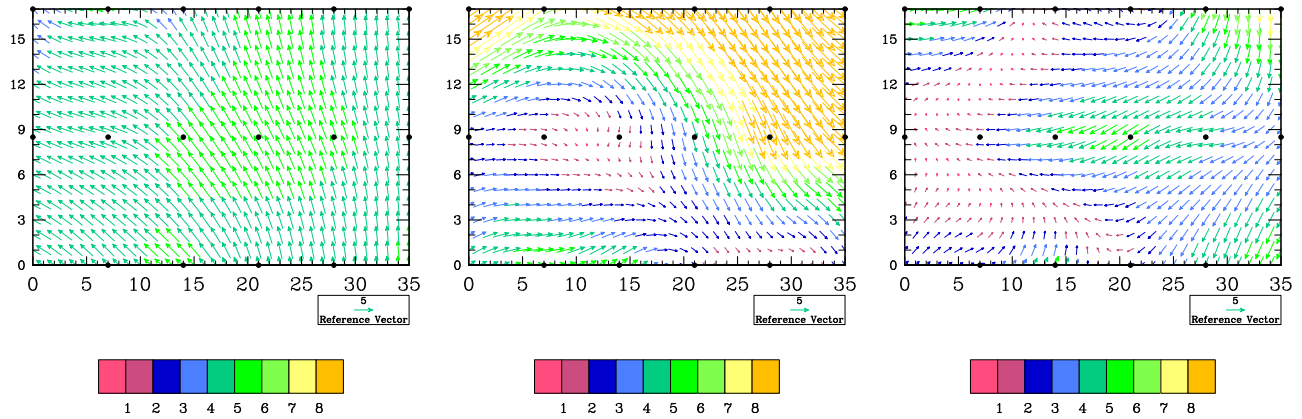


Figure 8: Ground network 10-minute average winds (m s^{-1}) interpolated on the regular north-south oriented grid. Black dots represent locations of the ground stations. Left panel: 12 PST (20 UTC) March 25; normal thermal circulation pattern. Middle panel: 17 PST March 25 (01 UTC March 26); strong westerly downslope winds. Right panel: 19 PST March 25 (03 UTC March 26), the footprint of the rotor.

The wind pattern in the valley constructed by interpolating the ground network measurements on a regular north-south oriented grid at three different times during March 25 is shown in Fig. 8. The three panels show respectively the wind field during a quiet period with the mid-day thermal circulation pattern around 12 PST, the westerly wind around 17 PST (time of the satellite image and photo in Fig. 4), and the footprint of the rotor around 19 PST. The easterly winds documented by the ground network at 19 PST are strongly suggestive of the rotor reaching the ground during this period.

3.d Wind Profiler Data

The MISS and MAPR wind profilers document this event through observations of periods of strong winds, large vertical motion, and increased spectral width which is related to turbulence.

Boundary layer wind profilers are not traditionally used to study waves and rotors, but can provide important clues to diagnose their presence, location, and strength. Figure 9 shows time-height cross sections of the vertical velocity (w) and spectral width (s) measured above MAPR at times surrounding IOP 8. Profiler performance may be limited by ground clutter and birds, and by low signal strength especially at higher altitudes. While w is normally less than about 1 m s^{-1} in the boundary layer, except perhaps for short periods within thermal plumes, the measurements during IOP 8 show many periods of persistent strong updrafts (red) and downdrafts (blue). See for example data above 2 km

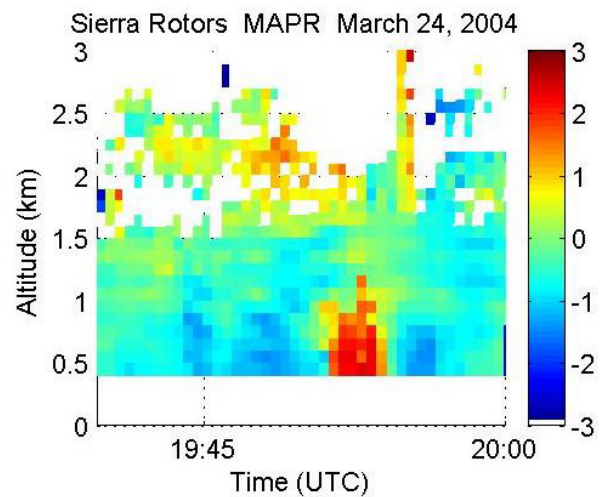


Figure 10: Strong updraft (red) observed at the start of IOP 8, coincident with the westerly flow observed by the surface network.

at 03 UTC and 07 UTC on March 27. Persistent vertical motion comes from gravity waves generated by strong flow over the upstream mountains. The sign and strength of the measurement greatly depends on the phase of the wave above the profiler location. The width of the Doppler spectrum, also shown in Fig. 9, represents velocity variation within the radar pulse volume during the integration period (typically about 30 s), and also is affected by the horizontal wind speed. Large spectral width is characteristic of turbulence which would be generated by rotors or wind shear. Spectral width is more

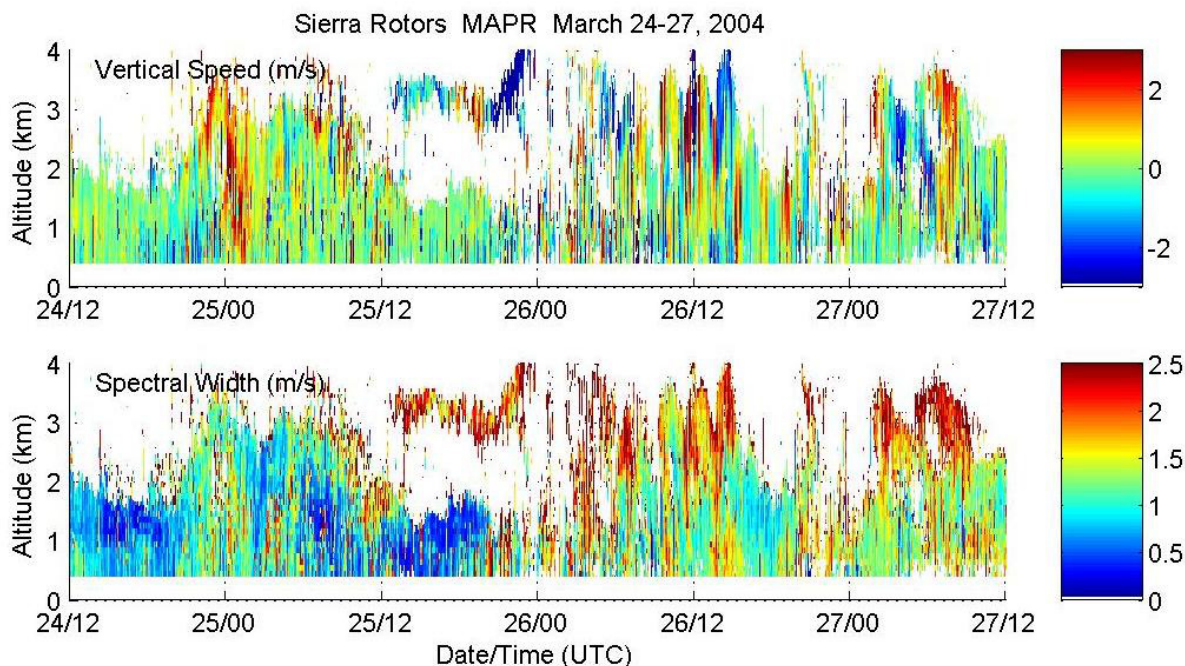


Figure 9: Time height cross section of vertical velocity and Doppler spectral width observed with MAPR for 72 hour period encompassing IOP 8 from 12 UTC on March 24 through 12 UTC on March 27. Altitudes are above ground level (AGL).

susceptible to measurement error than velocity, and more outliers are present.

We discuss three periods within IOP 8 to document events captured in the wind profiler data. First, close examination of w just before 20 UTC March 24, the time of the onset of strong westerly winds seen at the surface stations, shows an updraft exceeding 2 m s^{-1} for more than 3 minutes. This abrupt lifting is shown in Fig. 10 and is similar to past observations of gust fronts or density currents with MAPR. Notice that there is significant sinking of order 1 m s^{-1} both before and after the lifting. This event is followed by an observation of persistent large w aloft beginning around 22 UTC on March 24. This is the red region in Fig. 9 above 2.5 km. The persistent positive w continues through about 02 UTC (March 25) over the MAPR site and descends in altitude. During the same time period, the spectral width increases from typical (quiet) values less than 0.75 m s^{-1} (blue) to values of 1.25 m s^{-1} and greater (green and yellow).

Later on March 25 a second interesting phenomenon is seen. Alternating periods of positive and negative vertical motions exceeding 2 m s^{-1} are present in a reflective layer at 3 km from 13 to 23 UTC. Broad spectral widths of more than 2 m s^{-1} are also present in this layer. Turbulence enhances

atmospheric reflectivity, making this layer visible to MAPR. Although the signal strength weakens, and the measurements are less continuous, the broad widths are seen to continue into March 26. Examination of the profiler data at the time reverse flow is seen in the surface network, around 03 UTC (19 PST) on March 26 (March 25), shows that broad spectral widths have descended below 1 km. This supports the supposition that the easterly surface winds are caused by a rotor reaching the surface. The consistency between surface observations and wind profiler measurements gives us confidence that the profiler data can be used to extend observations of the rotor in altitude.

A final interesting period of wind profiler observations is around 12 UTC on March 26. There are large vertical velocities aloft, changing between positive and negative values quite abruptly. A closer look at a single altitude, 2.7 km, is shown in Fig. 11. Between 10:30–12:30 UTC, w goes from relatively small values, to updrafts of $3\text{--}6 \text{ m s}^{-1}$ persisting for more than 30 minutes, to a downdraft of 4 m s^{-1} , and then again becomes an updraft. During this period of large w , the spectral width is consistently about 2 m s^{-1} , indicating high winds or turbulence. A rawinsonde was launched from the MAPR site at 12 UTC. Figure 12 shows its ascent

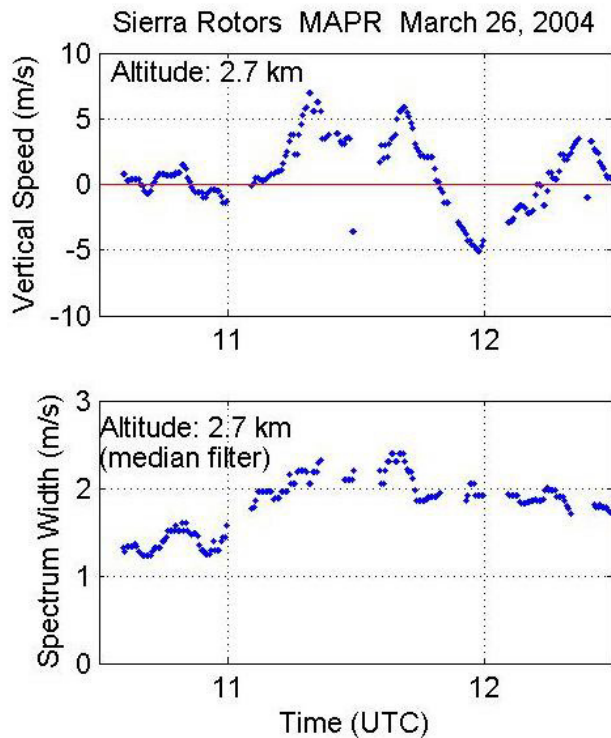


Figure 11: Time series of vertical velocity (top) and spectral width (bottom) from MAPR at 2.7 km AGL during a 2-hour period on March 26.

rate, which is radically modulated by these waves. Typical ascent rates are $4\text{--}5\text{ m s}^{-1}$ but above 1 km (AGL) this sonde accelerated to more than 10 m s^{-1} upward and then descended at more than 3 m s^{-1} for a time. This modification of the normal ascent rate indicates that the sonde passed through waves with vertical motion of about $\pm 4\text{ m s}^{-1}$.

4. SUMMARY

We have discussed preliminary findings for one of the rotor events (IOP 8) documented during the recently completed Special Observation Period of the Sierra Rotors Project in March and April 2004. Strong rotor events, such as this one, are expected to leave a marked footprint at the ground with strong easterly winds in the central part of the valley that was indeed detected by the ground network. The wind profilers showed strong wave activity and turbulence throughout the SOP, indicated by strong vertical motion and broad spectral width. The spectral width appears to support a rotor reaching the surface during the observed easterly winds.

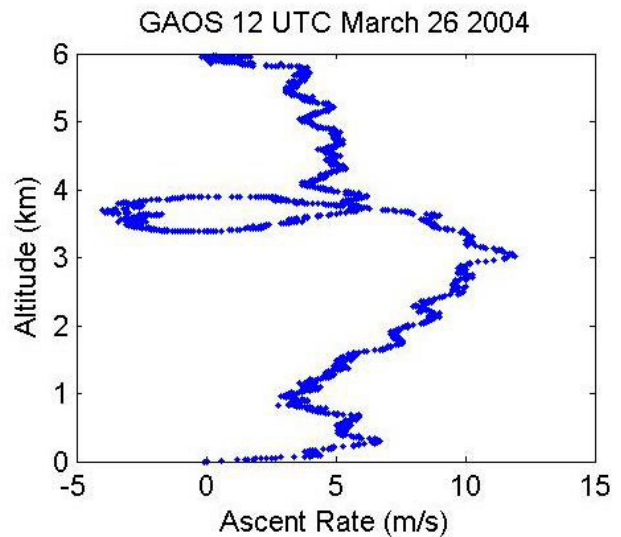


Figure 12: Ascent rate of the 12 UTC March 26 rawinsonde launched from MAPR. Normal ascent rates are about $4\text{--}5\text{ m s}^{-1}$, but wave activity alternately carried this sonde upward at more than 10 m s^{-1} and downward at nearly 5 m s^{-1} .

Acknowledgments. The success of field projects is secured through active collaboration of many individuals and organizations. We thank all those involved in the Sierra Rotors Project for their individual contributions to this project. The Sierra Rotors Project has been funded by the National Science Foundation. The first author was supported in part by the National Science Foundation (NSF), Division of Atmospheric Sciences, Grant ATM-0242886.

5. REFERENCES

- Cohn, S. A., W. O. J. Brown, C. L. Martin, M. S. Susedik, G. Maclean, and D. B. Parsons, 2001: Clear air boundary layer spaced antenna wind measurements with the Multiple Antenna Profiler (MAPR), *Annales Geophysicae*, **19**, 845–854.
- Cohn, S. A., H. B. Bluestein, W. O. J. Brown, and M. E. Susedik, 2004: The Mobile Integrated Sounding System (MISS): Description and First Results, *Preprints, 20th International Conference on Interactive Information Processing Systems (IIPS)*, Seattle, WA, Amer. Meteor. Soc., available on conference CD.
- Grubišić, V., and J. P. Kuettner, 2004: Sierra

Rotors and the Terrain-induced Rotor Experiment (T-REX) *Online Preprints. 11th Conference on Mountain Meteorology and the Annual Mesoscale Alpine Programme Meeting.* Amer. Meteor. Soc.

Parsons, D. B., and CoAuthors, 1994: The Integrated Sounding System: Description and preliminary observations from TOGA-COARE, *Bull. Amer. Meteor. Soc.*, **75**, 553–567.